Supporting Information for

Ionomer Side Chains Modulate Interfacial Microenvironments for Selective CO_2 Electrolysis

Jihyun Park,[1,2,†] Younghyun Chae,[1,3,†] Chanwoo Lee,[1,3] Gyeongjin Kwon,[1] Woong Hee Lee,[1,3] Hyo Sang Jeon,[4] Jinhan Cho,[2] Da Hye Won,[1,3,5,*] and Jai Hyun Koh[1,3,*]

[†]These authors contributed equally to this work.

[1]Clean Energy Research Center, Korea Institute of Science and Technology (KIST), Seoul 02792, Republic of Korea

[2]Department of Chemical and Biological Engineering, Korea University, Seoul 02841, Republic of Korea

[3]Division of Energy & Environment Technology, KIST School, University of Science and Technology, Seoul 02792, Republic of Korea

[4]Sustainable Energy Research Division, Korea Institute of Science and Technology (KIST), Seoul 02792, Republic of Korea

[5]KHU-KIST Department of Converging Science and Technology, Kyung Hee University, Seoul 02477, Republic of Korea

Corresponding Authors

*Email: dahye0803@kist.re.kr (D.H.W.); jhkoh@kist.re.kr (J.H.K.)

Table of Contents

1. Experimental

Materials. Styrene (≥99%), 4-vinylbenzyl chloride (VBC, 90%), 2-cyano-2-propyl dodecyl trithiocarbonate (CPDT, 97%), lauroyl peroxide (LPO), toluene (anhydrous, 99.8%), imidazole (>99%), potassium hydroxide (reagent grade, 90%, flakes), 1-bromobutane (99%), 1-bromodecane (98%), 1-bromohexadecane (97%), 1-methylimidazole (99%), Nafion solution (5 wt% in lower aliphatic alcohols and water), potassium bicarbonate (99.7%), deuterium oxide (D_2O, 99.9 atom% D, contains 0.05 wt.% 3-(trimethylsilyl)propionic-2,2,3,3-d_4 acid, sodium salt), and Sn nanopowder (Sn NP, >99%) were purchased from Sigma-Aldrich. Azobisisobutyronitrile (AIBN), aluminum oxide (5016-A, Basic, Brockmann Grade I), magnesium sulfate (anhydrous, 99.5% min), anhydrous $MgSO_4$ (99.5%), Ag nanopowder (Ag NP, APS 20–40 nm, 99.9%), and Iridium (IV) oxide (99%) were purchased from Alfa Aesar. Methanol (99.5%), *n*-hexane (99%), tetrahydrofuran (THF, 99.5%), dichloromethane (DCM, 99.8%), *N, N*-dimethylformamide (DMF, HPLC, 99.8%), ethyl acetate (EtOAc, 99.5%), diethyl ether (≥99%), and dimethyl sulfoxide (DMSO, 99.9%) were purchased from Daejung Chemicals. AIBN and LPO were recrystallized from methanol and *n*-hexane, respectively, prior to use. All chemicals and solvents were used without further purification unless stated otherwise.

RAFT Copolymerization of Styrene and VBC. The radical stabilizers in styrene and VBC were removed by passing through a basic Al_2O_3 column prior to polymerization. The statistical copolymers of styrene and VBC were synthesized by RAFT polymerization using AIBN and CPDT as the radical initiator and chain transfer agent, respectively. The general procedure is as follows: inhibitor-free styrene, VBC, AIBN, and CPDT were added to a 100 mL two-neck round-bottom flask charged with a stir bar and a rubber septum. Polymerization was conducted either with toluene as a solvent or without a solvent (i.e., bulk polymerization). The reaction mixture was vigorously purged with N_2 for at least 30 min and then heated at 70 ºC for 24 h. The reaction mixture was then quenched at 0 ºC and precipitated into methanol to yield a yellow powder. The crude polymer was isolated by filtration, dissolved in THF, and re-precipitated into methanol twice to remove the remaining monomers and impurities. The purified yellow powder was dried *in vacuo* at 60 ºC to yield poly(styrene-*co*-4-vinylbenzyl chloride) (P(S-*co*-VBC)). Three copolymer samples with different molecular weights were synthesized using the same procedure. The detailed reaction conditions are provided in Table S1.

Removal of CPDT End-group of P(S-*co*-VBC). The CPDT end-groups of the as-synthesized P(S-*co*-VBC) were removed using the slightly modified procedure from the literature.[1] P(S-*co*-VBC) was dissolved in toluene with LPO and AIBN. The reaction mixture was then heated at 80 ºC for 4 h with vigorous stirring. The solution was precipitated into methanol, filtered, and dried *in vacuo* at 60 ºC to yield a white powder. All three copolymer samples were subjected to the same procedure to remove the CPDT end-groups, in order to prevent unwanted chain transfer reactions.

Synthesis of 1-*n*-Alkylimidazoles.

1-n-Butylimidazole. Imidazole (3.00 g, 44.07 mmol) was mixed with potassium hydroxide (2.97 g, 52.88 mmol) in DMF (30 mL). 1-Bromobutane (6.40 g, 46.71 mmol) was added dropwise to the reaction mixture and stirred at 120 ºC for 16 h. The product was extracted with DCM. The organic layer was washed with water and brine, dried over anhydrous $MgSO_4$, and concentrated *in vacuo* to yield a 1-*n*-butylimidazole. The crude product was then purified using flash column chromatography to yield 1.40 g (26%) of the product as a pale yellow oil.[2]

1-n-Decylimidazole. 1-Bromodecane was used instead of 1-bromobutane. The rest of the procedure was the same as described above. 1-*n*-Decylimidazole was obtained as a very pale yellow oil.

1-n-Hexadecylimidazole. 1-Bromohexadecane was used instead of 1-bromobutane. The rest of the procedure was the same as described above. 1-*n*-Hexadecylimidazole was obtained as a white powder.

Functionalization of Styrene-based Copolymers with 1-*n*-Alkylimidazoles. The P(S-*co*-VBC) (1.3 g, 0.06 mmol) was dissolved in DMF (10 mL). To this solution, 1-*n*-alkylimidazole (5.7 mmol, 100 eq. relative to VBC units) was added. 1-*n*-alkylimidazoles used here were 1-methylimidazole, 1-*n*-butylimidazole, 1-*n*-decylimidazole, and 1-*n*-hexadecylimidazole. The reaction mixture was maintained at 110 ºC with vigorous stirring for 48 h. Subsequently, the ionomer was precipitated into diethyl ether, filtered, and dried overnight *in vacuo* at 60 ºC to give a brown solid.[3]

Preparation of Catalysts and Electrodes. Ag NPs (10 mg) were dispersed in ethanol (1 mL) and sonicated for 30 min. This dispersion was then mixed with the prepared ionomer (10 mg) in methanol (2 mL) and stirred until fully dissolved, forming the catalyst ink. The catalyst ink solution was sprayed onto Sigracet 39BB GDL (SGL carbon) using a spray gun (Gunpiece GP-2, Fuso Seiki) until the total loading amount reached 1 mg cm^{-2}, which was determined from the difference in the weight of electrodes before and after spraying. The substrate was subsequently floated on a 1 M KOH solution for 1 h, washed with water, and dried at room temperature to activate the ionomer.

For long-term operation, the carbon-reinforced electrode was prepared by adding Ketjen Black 600J (5 mg) to ethanol (2 mL) and then mixing it with the ink of Ag and ionomer (C16-20k). The loading amount for the carbon-reinforced electrode was 1.3 mg cm^{-2}. After spraying, the electrode was activated following the identical procedure described above.

Two-compartment Cell (H-Cell). The geometric surface areas of the electrodes were 0.5 cm^2, and the rest of the substrate was covered with silicone tape. Platinum foil and Ag/AgCl (3 M KCl) were used as the counter and reference electrodes, respectively.

Membrane Electrode Assembly (MEA). The geometric surface areas of the electrodes were 5 cm^2. Iridium(IV) oxide was used as the catalyst for the anode. Typically, 30 mg of iridium oxide was dispersed in 1 mL of isopropyl alcohol and sonicated for 30 min. This dispersion was then mixed with 30 mg of Nafion solution (5 wt%) to form a catalyst ink for the anode. The resulting ink was sprayed onto a platinized titanium mesh until the loading amount of iridium oxide reached 1 mg cm^{-2}. The geometric surface area of the anode was adjusted to 6.25 cm^2.

Electrochemical CO_2 Reduction Reaction (CO_2RR).

H-Cell. CO_2RR experiments were conducted using a potentiostat (Iviumstat, Ivium Technologies) in a custom three-electrode H-cell, with a Selemion AMV-N (Asahi Glass) membrane for the separation of catholyte and anolyte. The electrolyte solutions were purged with CO_2 (99.999%) for 1 h, and the pH of the electrolytes was subsequently measured with a pH meter. The electrochemical CO_2 reduction reactions were performed using chronoamperometry at fixed potentials, which were converted to the reversible hydrogen electrode (RHE) scale with 85% iR compensation using the following equation:

$$V_{RHE} = V_{Ag/AgCl} + 0.197\ \text{V} + 0.059\ \text{V} \times \text{pH} + 0.85 \times iR_s \quad (1)$$

where i stands for current and R_s represents resistance measured by electrochemical impedance spectroscopy (EIS). The anodic reaction was the oxygen evolution reaction (OER), catalyzed by a Pt foil electrode in aqueous electrolyte, serving as the counter reaction to cathodic CO_2RR.

MEA. A CO_2 electrolyzer (Dioxide Materials) with an active area of 5 cm^2 was employed for measurements of electrochemical performance. Chronoamperometry was conducted at room temperature using a two-electrode configuration, with voltages applied stepwise to the full cell. The zero-gap electrolyzer consisted of a cathode, an anode, and a Nafion 211 membrane for the exchange of cations. EIS was performed before and after the chronoamperometry measurements to monitor cell resistance, confirming the maintenance of the zero-gap configuration. The channel for the anolyte was designed with a serpentine flow path, through which 150 ml of 0.1 M $KHCO_3$ solution was continuously circulated at 20 mL min^{-1} using a peristaltic pump (EMS-Tech). A humidified gas stream of CO_2 at 100% relative humidity and 30 ºC was supplied to the cathodic channel at a flow rate of 100 sccm using a mass flow controller (Bronkhorst EL-FLOW). The anodic reaction was the oxygen evolution reaction (OER), which corresponds to the half-cell reaction of water electrolysis, and was catalyzed by an IrO_x catalyst.

For the evaluation of the long-term performance and durability of the MEA, C16-20k was selected as a representative ionomer, and electrolysis was performed for 9 h at a cell voltage of 3.0 V with 0.1 M $KHCO_3$ as the anolyte. Carbon black (Ketjen Black 600J, 50 wt% relative to Ag) was incorporated into the electrode to enhance operational stability by preventing the precipitation of salts and reinforcing the integrity of the electrode. The electrode containing C16-20k maintained stable performance throughout the 9-h electrolysis (Figure S16), surpassing previously reported 6-h durability for a similar CEM-based configuration employing Sustainion XA-9 ionomer and carbon black.[4] The consistent electrochemical performance strongly indicates the intrinsic durability of the ionomer under prolonged electrolysis conditions.

Analysis of Products. Gas chromatography (GC, 7890B, Agilent Technologies) with a flame ionization detector (FID) and a thermal conductivity detector (TCD) with a methanizer were used to analyze the gas products. A ShinCarbon ST 100/120 (2 m, 1 mm ID, Restek) column and Ar (99.9999%) were used for the GC as the column and the carrier gas, respectively. Gas samples from the cathodic outlet were collected and analyzed 15 min after the reaction started. The gas evolved from the anodic reaction was assumed to be stoichiometric amount of oxygen corresponding to the applied current, and thus no further analysis was conducted. The liquid products were analyzed using ^{1}H Nuclear Magnetic Resonance (NMR) spectroscopy (Avance III HD 400, Bruker) with H_2O suppression, using D_2O as the lock solvent and internal reference. Liquid samples were collected immediately after the 30-minute experiment for the H-type cell. The average CO_2 flow rate was 24 mL min^{-1}, measured using a flow meter (ADM 2000, Agilent Technologies) at the GC outlet. The productivity of each product from the CO_2RR was converted to Faradaic efficiency (FE). The FEs of the products were calculated as the ratio of the partial current of each product to the total current using the following equations:

$$FE_{product}(\%) = \frac{i_{product}}{i_{total}} \times 100 = \frac{mole_{product} \times F \times N}{i_{total}} \times 100 \quad (2)$$

where $mole_{product}$ is the actual number of moles of the product quantified by GC or NMR, F is the Faraday constant (96,485 C mol^{-1}), and N is the number of electrons consumed to produce each product from CO_2. All cathodic current densities were expressed without minus signs.

Preparation of Electrolytes with Different Compositions. Two sets of electrolytes were prepared to investigate the influence of side chain length of ionomers under different electrolyte compositions. These sets provided bulk solutions with different (1) [HCO_3^-] and (2) pH. Electrolytes containing K^+ ions, such as K_2HPO_4 and K_2SO_4, were added to maintain a consistent K^+ concentration while adjusting [HCO_3^-] and pH. Each electrolyte was prepared by dissolving the required amounts of $KHCO_3$, K_2HPO_4, K_2SO_4, or H_2SO_4 in deionized water under continuous stirring until fully dissolved. Each solution was then saturated with CO_2 by bubbling CO_2 gas at a controlled flow rate for at least 30 minutes before use. Fresh solutions were prepared before each experiment to ensure consistency and stability. This approach ensured that variations in CO_2RR activity and selectivity were attributed to differences in [HCO_3^-] and pH rather than fluctuations in K^+ concentration, which influences CO_2 reduction.[5]

Variations in HCO_3^- Concentrations. Three electrolytes with different HCO_3^- concentrations were prepared with the following compositions: 1.0 M, 0.5 M, and 0.1 M HCO_3^-. Only $KHCO_3$ was used for the preparation of 1.0 M HCO_3^-. For the 0.5 M HCO_3^- electrolyte, 0.5 M $KHCO_3$ and 0.25 M K_2HPO_4 were dissolved, while for the 0.1 M HCO_3^-, 0.1 M $KHCO_3$ and 0.45 M K_2HPO_4 were used. The addition of K_2HPO_4 instead of diluting $KHCO_3$ ensured that the total K^+ concentration remained constant across all solutions. Despite significant differences in HCO_3^- concentration, all three electrolytes showed similar bulk pH values after CO_2 saturation, confirming that pH was not a significant variable in this study.

Variations in pH. Two electrolytes with different pH values were prepared: a neutral solution at pH 6.8 and an acidic solution at pH 3.1. The neutral electrolyte consisted of a CO_2-saturated 0.1 M $KHCO_3$ solution. The acidic electrolyte was prepared by adding the mixture of a CO_2-saturated 0.05 M K_2SO_4 and 0.05 M H_2SO_4 to a CO_2-saturated 0.1 M $KHCO_3$ until the pH reached 3.1. The pH of the solution was measured with a pH meter (SevenCompact, Mettler Toledo). The addition of K_2SO_4 instead of simply acidifying $KHCO_3$ with H_2SO_4 ensured that the total K^+ concentration remained constant across all solutions.

Ionic Conductivity Measurements. The ionic conductivity (σ) of ionomers was measured by electrochemical impedance spectroscopy (EIS, Biologic VMP3B-10) in a Swagelok-type cell with two stainless steel electrodes. Each ionomer sample (58 mg) was prepared at a 5 wt% concentration in anhydrous DMSO (1.1 g). The ionomer solution was loaded into the Swagelok cell to measure the solution resistance (R_s) by EIS in the frequency range of 1 MHz to 5 Hz. Ionic conductivity in chloride form was calculated using the following equation:

$$\sigma = \frac{L}{R_s \times A}$$

where L is the distance between the two electrodes of the Swagelok-type cell, and A (1.99 cm^2) is the cross-sectional area of each electrode.

Gel Permeation Chromatography (GPC). The molecular weight and dispersity of a polymer were determined by GPC. The GPC traces were collected using a Jasco LC-4000 Series high-performance liquid chromatography (HPLC) system equipped with a Jasco RI-4030 refractive index (RI) detector and three Shodex columns (KF-802.5, KF-803, KF-804). THF was used as the eluent with a flow rate of 1.0 ml min^{-1} at 40 ºC. The column set was calibrated with polystyrene standards.

^{1}H Nuclear Magnetic Resonance (NMR) Spectroscopy. All synthesized polymers were characterized by ^{1}H NMR spectroscopy at 400 MHz using a Bruker Ascend or Avance III HD spectrometer. The polymers were dissolved in either $CDCl_3$ or DMSO.

Differential Scanning Calorimetry (DSC). DSC was performed using a TA Instruments DSC Q200 equipped with an SP Industries FC100 cooling system. The measurements were performed in a temperature range from 40 ºC to 200 ºC at a heating rate of 10 ºC min^{-1} under N_2. The T_gs were determined at the midpoints of the heat flow changes during the third cycle.

Thermogravimetric Analysis (TGA). TGA was performed using a TA Instruments SDT-Q600 under N_2. The samples were heated from room temperature to 800 ºC at a ramp rate of 10 ºC min^{-1}.

X-ray Diffraction (XRD). X-ray diffraction (XRD) spectra of Ag NPs and Sn NPs were recorded using Rigaku 27 Model D/MAX22. The measurements were performed with a scanning rate of 0.05 deg s^{-1}. Phase identification and peak assignment were conducted using the Jade software package, with reference to standard JCPDS files.

X-ray Photoelectron Spectroscopy (XPS). X-ray photoelectron spectroscopy (XPS) was performed on a Nexsa (Thermo Fisher Scientific) with Al Kα radiation. Ag $3d_{5/2}$ photoelectron peak (368.21 eV) was used for the calibration of the binding energy scale. All of the spectra were normalized to the maximum. Deconvolution of the XPS spectra was performed using the CasaXPS software with a Shirley baseline subtraction.

Scanning Electron Microscopy (SEM). The surface morphology and elemental composition of Ag NP electrodes with ionomer and Sn NP electrodes with ionomer were investigated using SEM (Inspect F or Inspect F50) equipped with an EDS at an acceleration voltage of 15.0 kV and a typical working distance of 10.0 mm. SEM energy dispersive X-ray (SEM-EDX) spectroscopy indicated that the Ag and Sn catalysts, together with the ionomers, were well-dispersed across the electrode surface (Figures S5 and S12, respectively). SEM images of Ag-ionomer electrodes confirmed that the surface morphology remained unchanged throughout electrode activation and subsequent CO_2RR experiments (Figure S27).

Transmission Electron Microscopy (TEM). The morphology and crystal structures of catalyst NPs were analyzed by a TEM (Tecnai, F20G2) operated at an accelerating voltage of 200 kV. TEM images were captured and processed using a Gatan CCD camera system and DigitalMicrograph software. The lattice fringe spacing was calculated by dividing the total length spanning 10 fringes by 10.

Water Contact Angle (CA) Analysis. Contact angles of water droplets were measured on ionomer-coated Ag NP electrodes using a microscope-coupled goniometer (Phoenix 150, SEO).

Water Uptake and Swelling Ratio. Water uptake and swelling ratio were measured based on changes in the weight (w) and thickness (t) of ionomer films, respectively. The ionomer films were prepared by dissolving each ionomer sample (63.4 mg) in DMSO (3.6 mL), casting the solution onto a substrate, and subsequently drying overnight at 60 ºC in a vacuum oven. The dried films were immersed in deionized water at room temperature for 1 h. The water uptake and swelling ratio were determined after removing surface water using the following equations:

$$\text{Water uptake } (\%) = \frac{w_{wet} - w_{dry}}{w_{dry}} \times 100$$

$$\text{Swelling ratio } (\%) = \frac{t_{wet} - t_{dry}}{t_{dry}} \times 100.$$

2. Supporting Figures and Tables

Table S1. RAFT copolymerization conditions and characterization of the P(S-*co*-VBC).

Polymer	Initiator/CTA	Time (h)	Conv.[d] (%)	M_n[e] (kg mol^{-1})	M_w/M_n[e]	Composition[f] (%)
P(S-*co*-VBC) 7k[a]	AIBN/CPDT	24	56	6.9	1.16	65% PS, 35% VBC
P(S-*co*-VBC) 20k[b]	AIBN/CPDT	24	25	20.1	1.46	65% PS, 35% VBC
P(S-*co*-VBC) 42k[c]	AIBN/CPDT	24	33	42.5	1.43	65% PS, 35% VBC

[a][S]$_0$:[VBC]$_0$:[I]$_0$:[CTA]$_0$ = 118:51:0.1:1, the polymerization was carried out in bulk at 70 ºC;
[b][S]$_0$:[VBC]$_0$:[I]$_0$:[CTA]$_0$ = 590:253:0.1:1, the polymerization was carried out in bulk at 70 ºC;
[c][S]$_0$:[VBC]$_0$:[I]$_0$:[CTA]$_0$ = 1,179:505:0.1:1, the polymerization was carried out in toluene at a total monomer concentration of 83.6 wt% at 70 ºC;
[d]Conversion was calculated by ^{1}H NMR analysis;
[e]Molecular weight and dispersity were determined by GPC based on calibration with PS standards;
[f]Copolymer composition was calculated by ^{1}H NMR analysis.

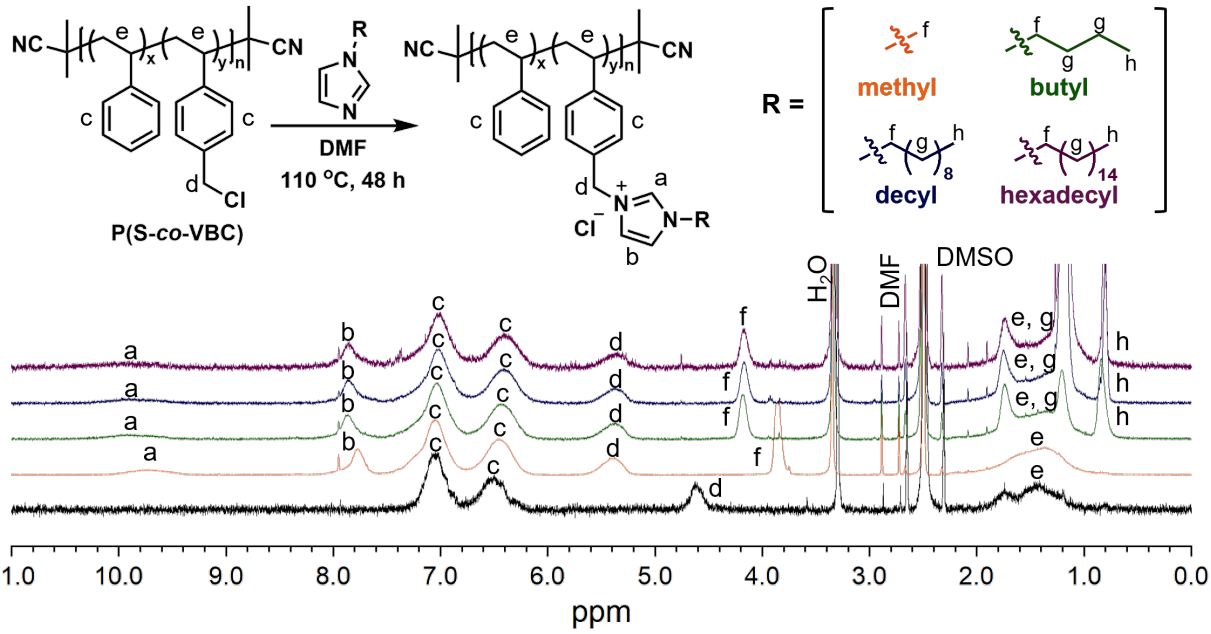

Figure S1. Representative ^{1}H NMR spectra for P(S-*co*-VBC) and a series of 1-*n*-alkylimidazolium (C_nH_{2n+1} where n = 1, 4, 10, and 16) ionomers in DMSO−d_6.

Table S2. Properties of the 1-*n*-alkylimidazolium ionomers synthesized from the P(S-*co*-VBC) of 20 kg mol^{-1}.

Ionomer	IEC (meq g^{-1})[a]	Ionic conductivity, σ (mS cm^{-1})[b]	σ/IEC (g S cm^{-1} eq^{-1})
C1-20k	2.44	0.8	0.33
C4-20k	2.21	0.65	0.29
C10-20k	1.87	0.60	0.32
C16-20k	1.61	0.51	0.32

[a]IEC was determined by ^{1}H NMR in chloride form;
[b]Ionic conductivity was measured at 5 wt% in anhydrous DMSO.

Table S3. Properties of the 1-*n*-hexadecylimidazolium (C16) ionomers synthesized from P(S-*co*-VBC)s of different molecular weights: 7, 20, and 42 kg mol^{-1}.

Ionomer	IEC (meq g^{-1})[a]	Ionic conductivity, σ (mS cm^{-1})[b]	σ/IEC (g S cm^{-1} eq^{-1})
C16-7k	1.61	0.39	0.24
C16-20k	1.61	0.51	0.32
C16-42k	1.61	0.38	0.24

[a]IEC was determined by ^{1}H NMR in chloride form;
[b]Ionic conductivity was measured at 5 wt% in anhydrous DMSO.

Table S4. Water uptake and swelling ratio of the 1-*n*-alkylimidazolium ionomers synthesized from the P(S-co-VBC) of 20 kg mol^{-1}.

Ionomer	Water uptake (%)	Swelling ratio (%)
C1-20k	77.8	9.2
C4-20k	50.0	5.3
C10-20k	23.5	2.6
C16-20k[a]	–	–

[a] Measurements unavailable; films were too brittle and fragmented.

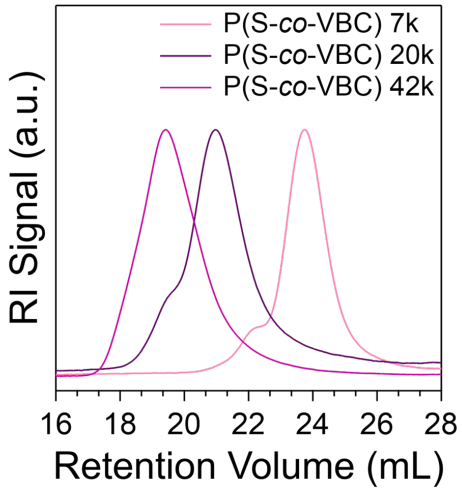

Figure S2. Gel permeation chromatography (GPC) traces of three P(S-*co*-VBC) samples synthesized and used in this study. The molecular weight and dispersity are shown in Table S1.

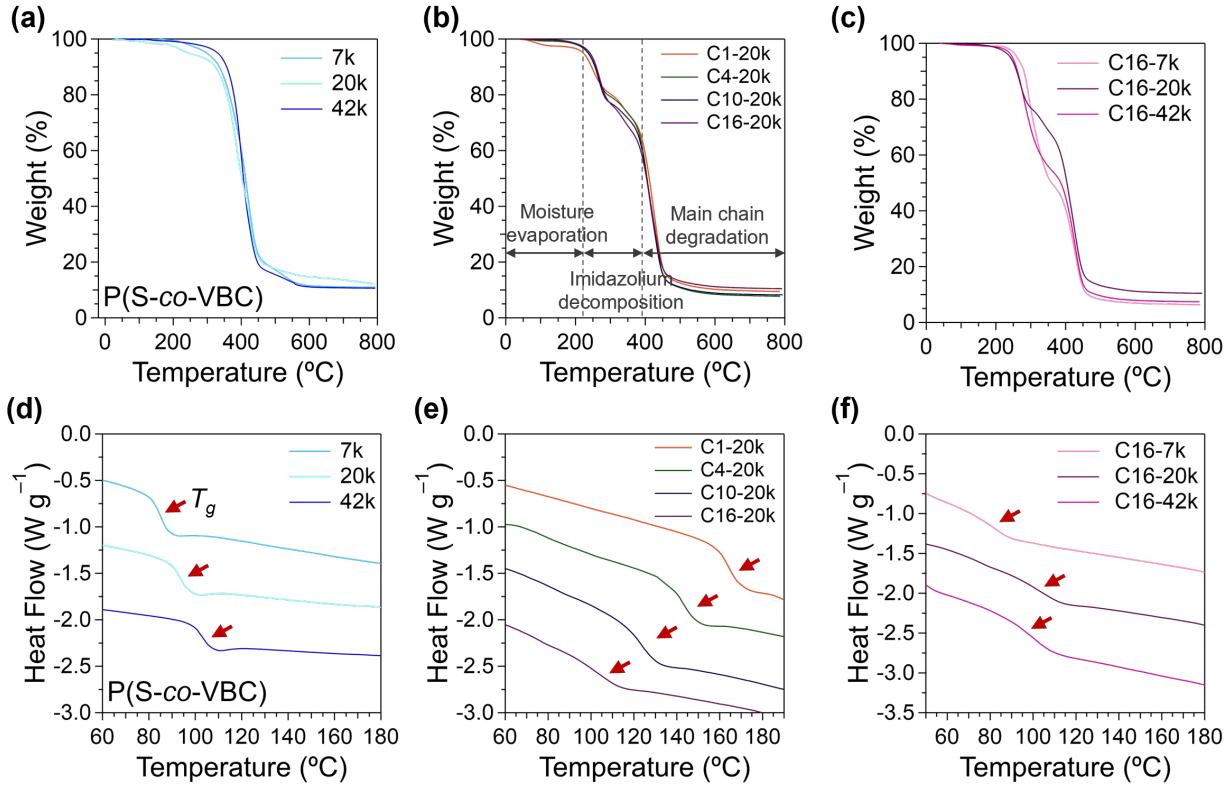

Figure S3. Thermal analyses of the P(S-*co*-VBC)s with different molecular weights (7, 20, and 42 kg mol^{-1}) and 1-*n*-alkylimidazolium ionomers with varying lengths of alkyl side chains (C1, C4, C10, and C16). (a–c) TGA curves and (d–f) DSC traces for: (a,d) P(S-*co*-VBC) 7k, 20k, and 42k; (b,e) C1-, C4-, C10-, and C16-20k; (c,f) C16-7k, -20k, and -42k.

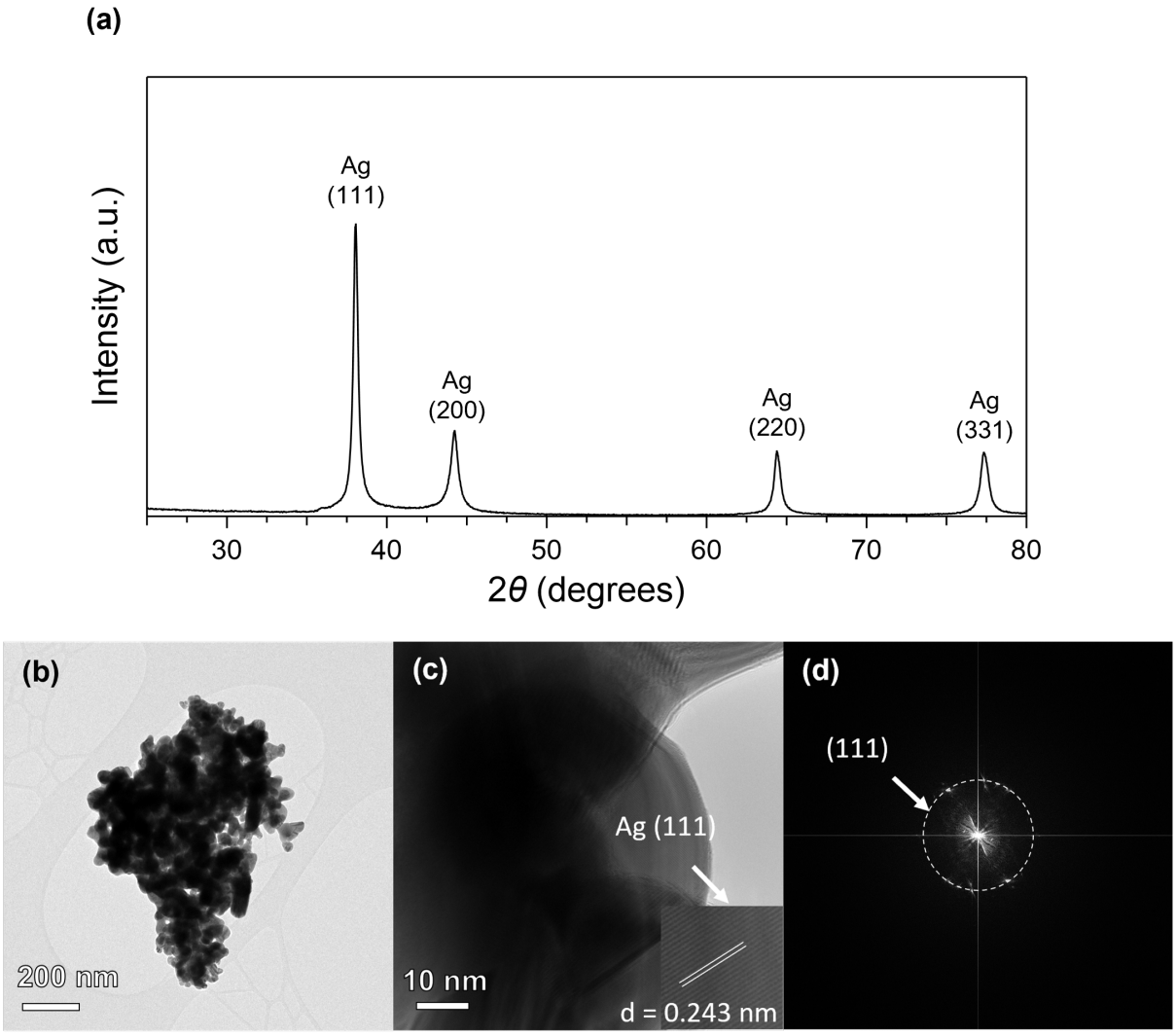

Figure S4. Characterization of the Ag NPs. (a) XRD patterns, (b) TEM, (c) HR-TEM, and (d) fast Fourier transform (FFT) images. The predominant presence of the Ag(111) peak in the XRD patterns is consistently observed in the HR-TEM images, with the circular appearance of Ag(111) evident in the FFT pattern as well. This indicates that the Ag NPs are polycrystalline materials. Peak analysis by XRD was conducted with reference to Ag (JCPDS Card No. 87-0720). The 2θ values for the (111), (200), (220), and (311) planes of Ag were assigned at 38.11º, 44.28º, 64.43º, and 77.40º, respectively.

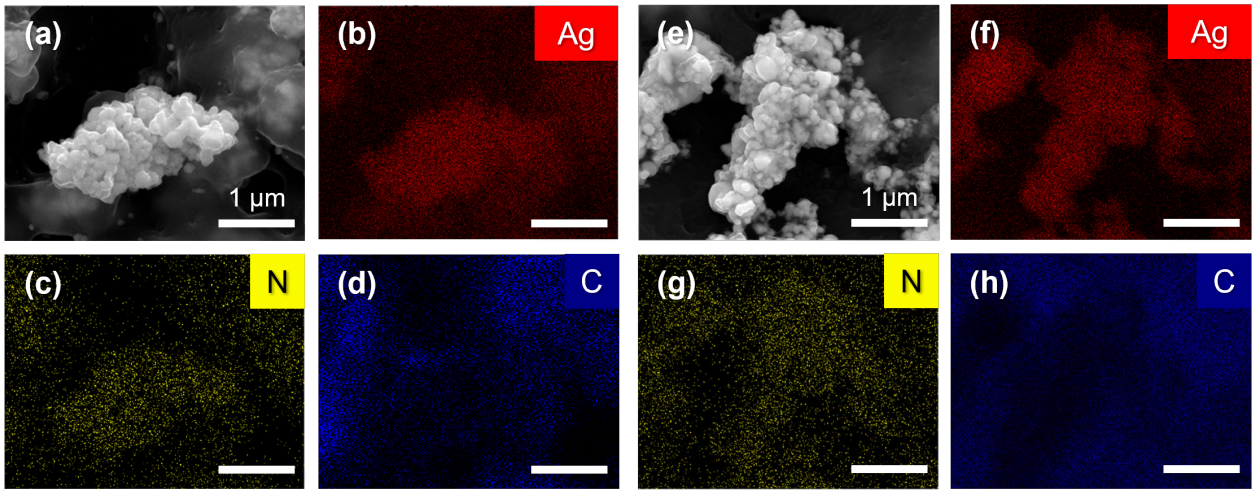

Figure S5. SEM images of electrodes coated with Ag NPs and C16-20k (a) before and (e) after CO_2RR (scale bar = 1 μm). The corresponding elemental mapping (EDS) images of (b,f) Ag, (c,g) N, and (d,h) C.

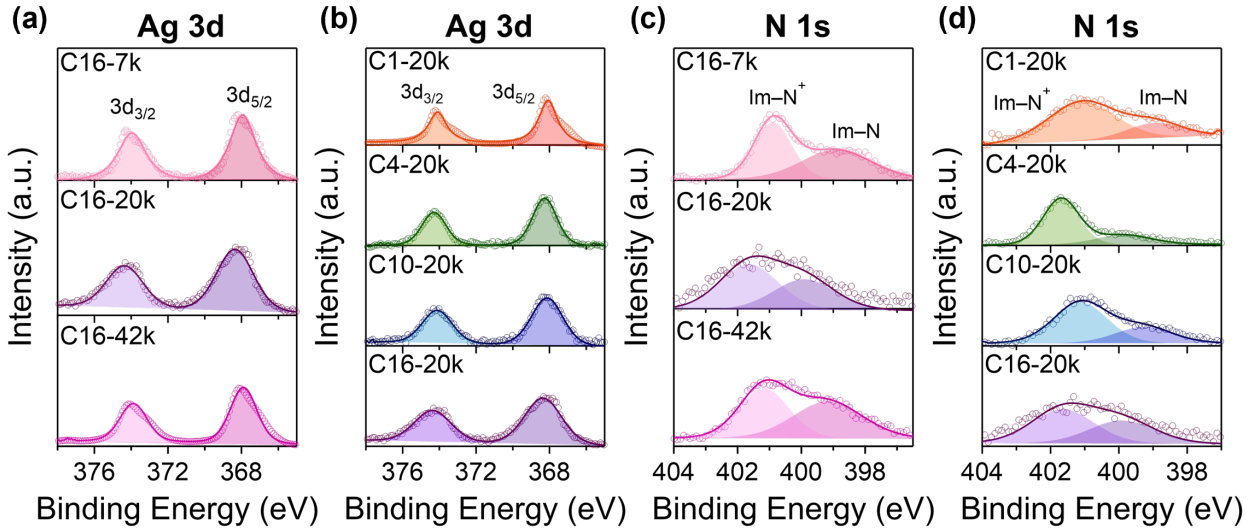

Figure S6. XPS spectra of all the electrodes coated with Ag NPs and 1-*n*-alkylimidazolium ionomers in the (a,b) Ag 3d and (c,d) N 1s regions: (a,c) C16-7k, -20k, and -42k; (b,d) C1-, C4-, C10-, and C16-20k.

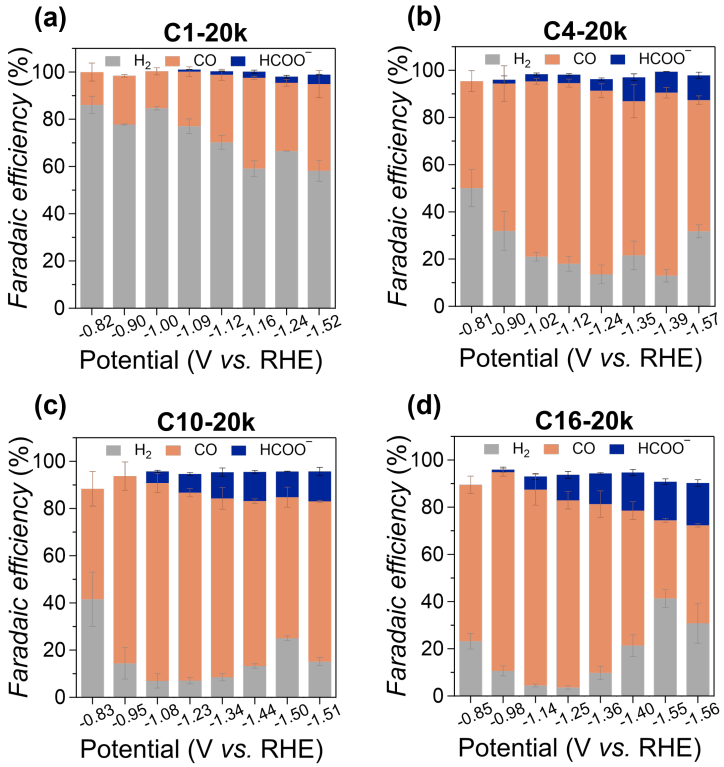

Figure S7. FE_{H_2} (gray), FE_{CO} (orange), and FE_{HCOO^-} (blue) on Ag-based electrodes coated with 1-*n*-alkylimidazolium ionomers: (a) C1-20k, (b) C4-20k, (c) C10-20k, and (d) C16-20k.

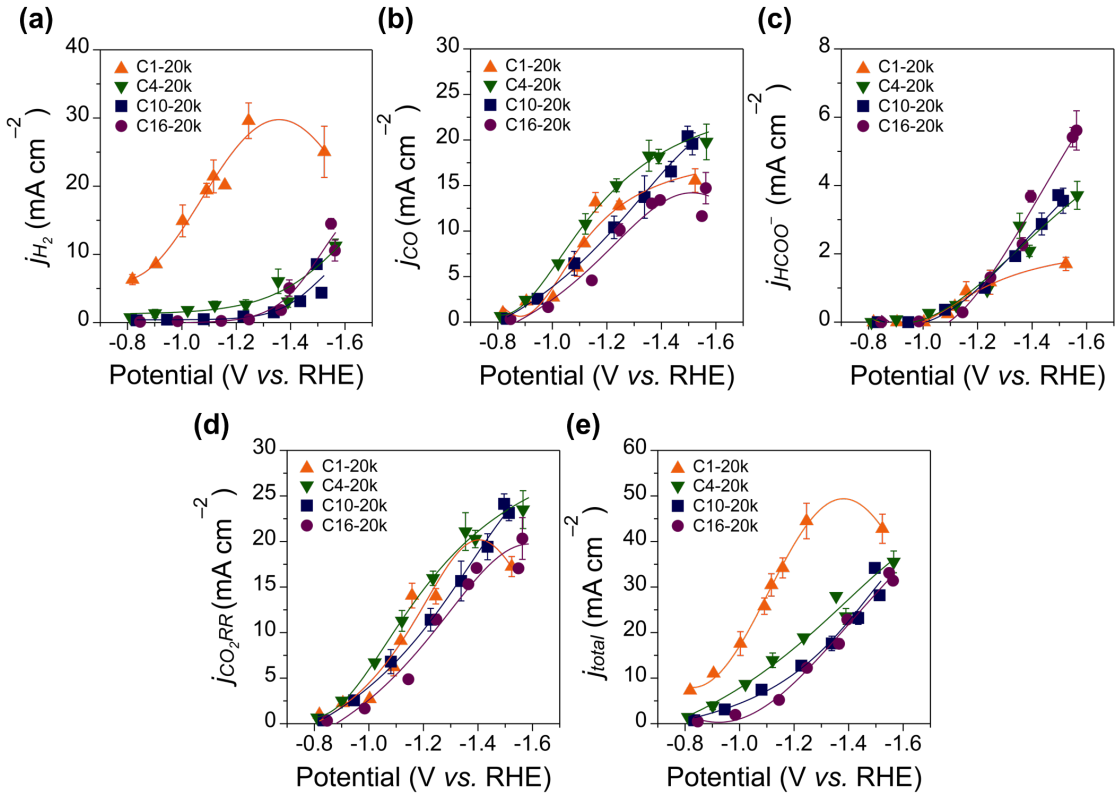

Figure S8. (a) j_{H_2}, (b) j_{CO}, (c) j_{HCOO^-}, (d) j_{CO_2RR}, and (e) j_{total} using C1-20k (orange, triangle), C4-20k (green, reverse triangle), C10-20k (blue, square), and C16-20k (purple, circle).

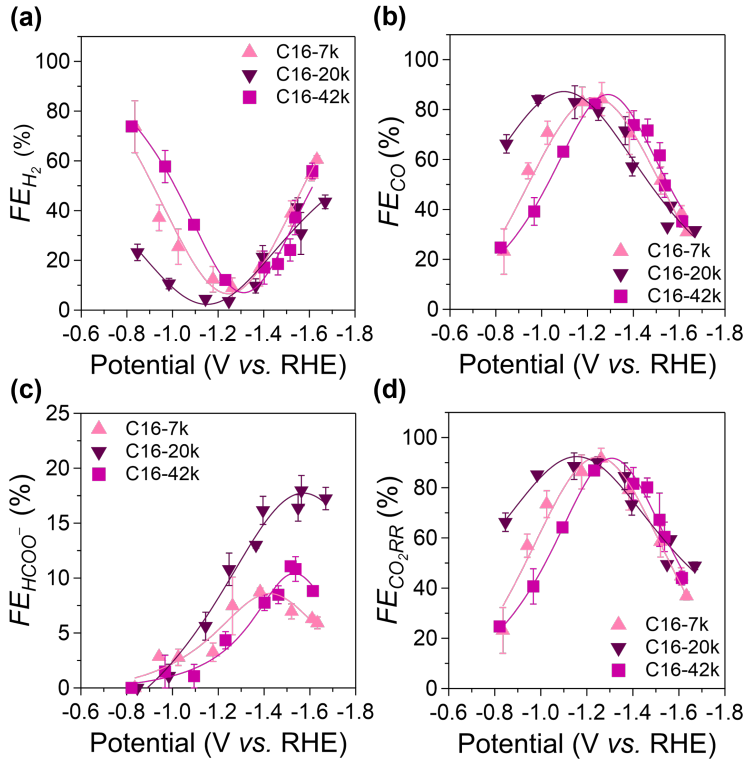

Figure S9. (a) FE_{H_2}, (b) FE_{CO}, (c) FE_{HCOO^-}, and (d) FE_{CO_2RR} for Ag-catalyzed CO_2RR using C16 ionomers of varying molecular weights: C16-7k (light pink, triangle), C16-20k (purple, reverse triangle), and C16-42k (magenta, square).

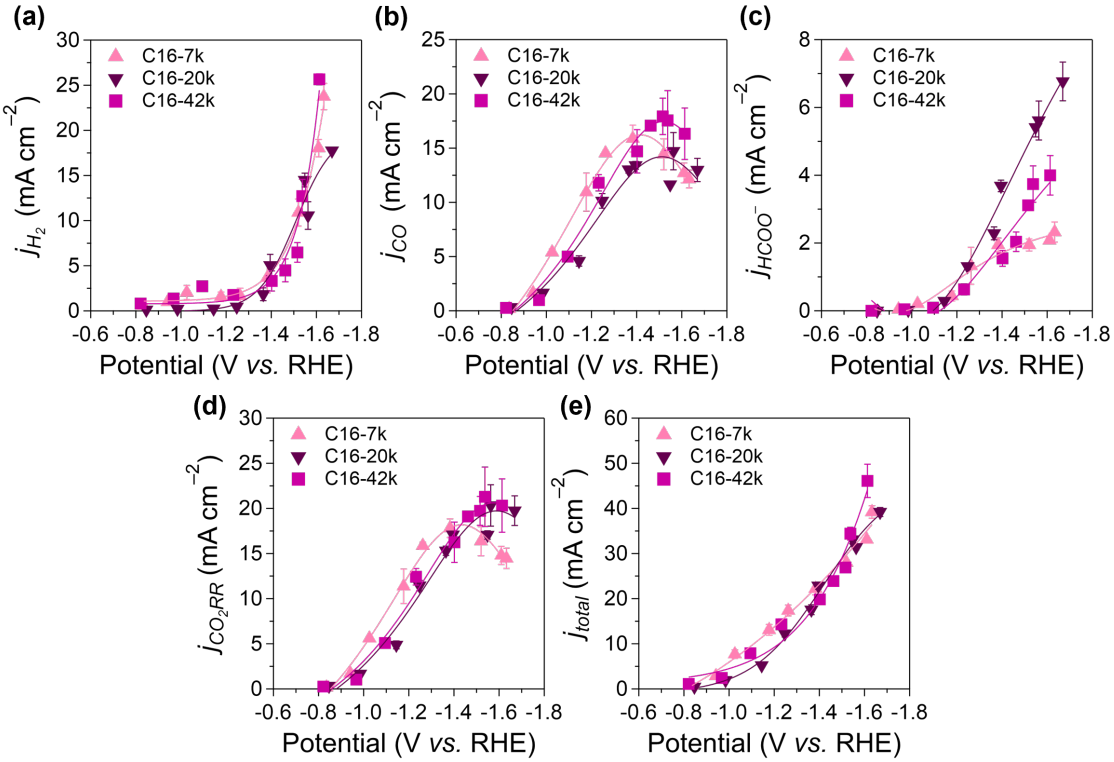

Figure S10. (a) j_{H_2}, (b) j_{CO}, (c) j_{HCOO^-}, (d) j_{CO_2RR}, and (e) j_{total} for Ag-catalyzed CO_2RR using C16 ionomers of varying molecular weights: C16-7k (light pink, triangle), C16-20k (purple, reverse triangle), and C16-42k (magenta, square).

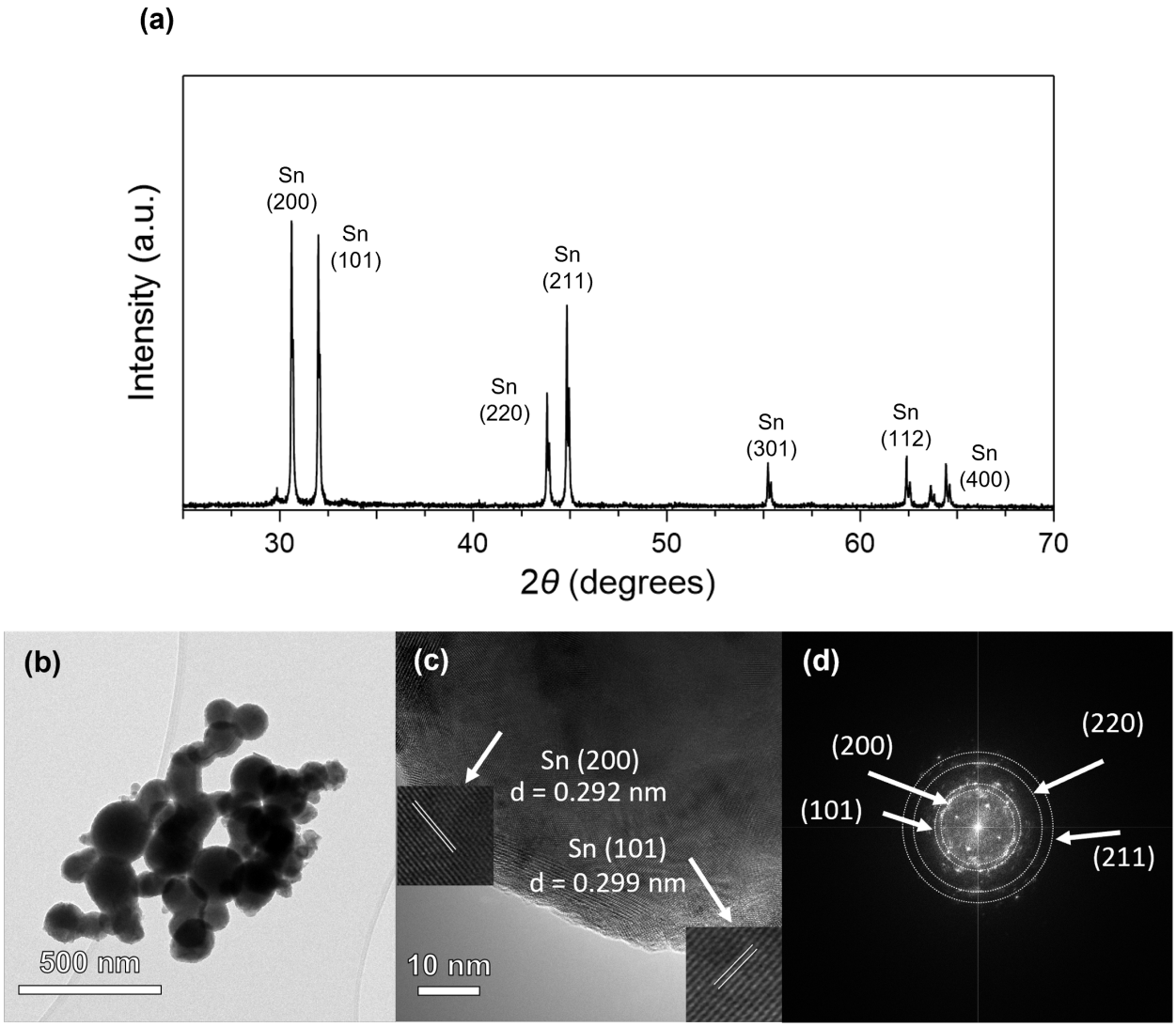

Figure S11. Characterization of the Sn NPs. (a) XRD patterns, (b) TEM, (c) HR-TEM, and (d) FFT images of Sn NPs. The predominant presence of the Sn(200) and (101) peaks in the XRD patterns is consistently monitored in the HR-TEM images, with the circular appearance of Sn(200), (101), (220), and (211) evident in the FFT pattern as well. This indicates that the Sn NPs are polycrystalline materials. Peak analysis by XRD was performed with reference to Sn (JCPDS Card No. 01-0926). The 2θ values for the (200), (101), (220), (211), (301), (112), and (400) planes of Sn were indexed at 30.62º, 32.02º, 43.80º, 44.55º, 55.97º, 62.60º, and 63.82º, respectively.

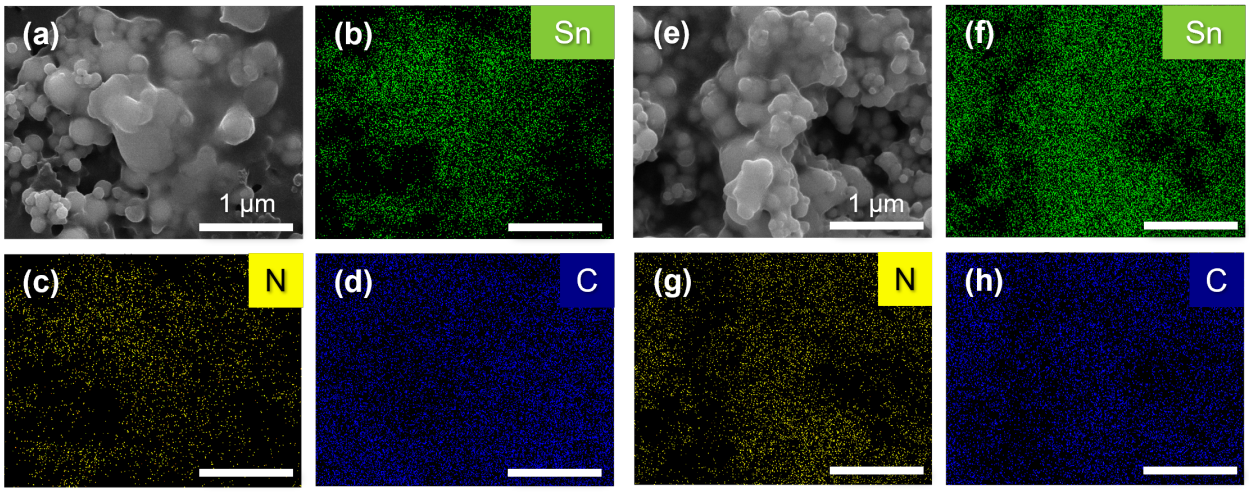

Figure S12. SEM images of electrodes coated with Sn NPs and the ionomers (a) C1-20k and (e) C16-20k, respectively (scale bar = 1 μm). The corresponding elemental mapping (EDS) images of (b,f) Sn, (c,g) N, and (d,h) C.

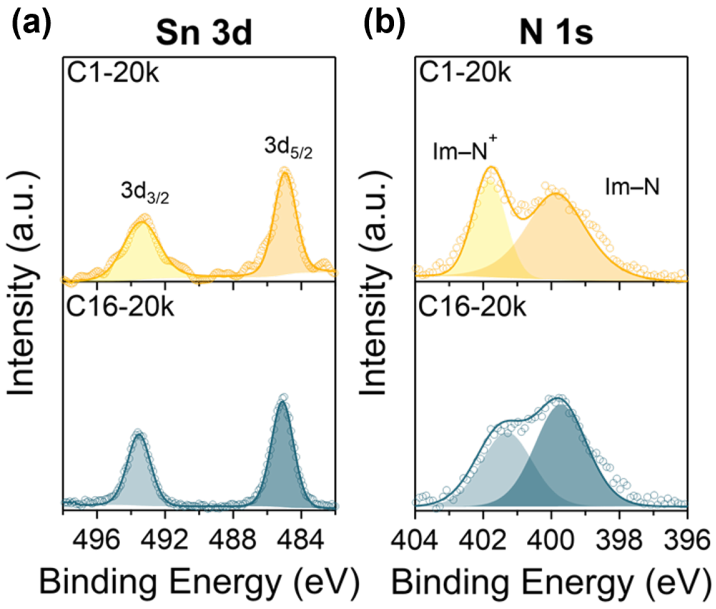

Figure S13. XPS spectra of electrodes coated with Sn NPs and the ionomers C1-20k and C16-20k, respectively, in the regions corresponding to (a) Sn 3d and (b) N 1s.

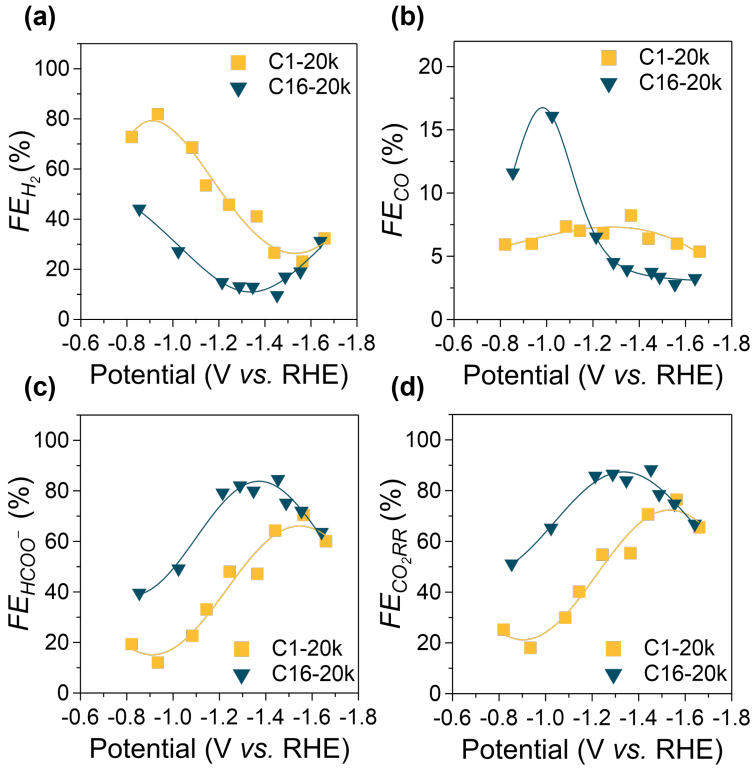

Figure S14. (a) FE_{H_2}, (b) FE_{CO}, (c) FE_{HCOO^-}, and (d) FE_{CO_2RR} for Sn-catalyzed CO_2RR using the C1-20k (yellow, square) and C16-20k (blue, reverse triangle).

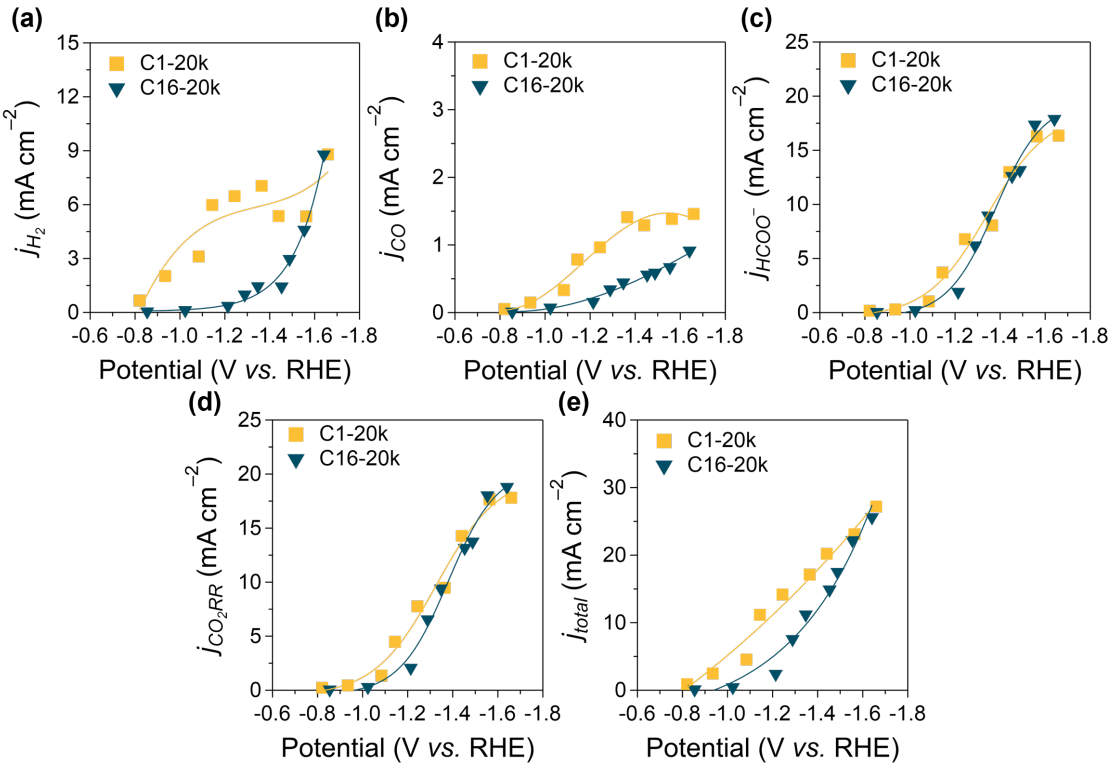

Figure S15. (a) j_{H_2}, (b) j_{CO}, (c) j_{HCOO^-}, (d) j_{CO_2RR}, and (e) j_{total} for Sn-catalyzed CO_2RR using the C1-20k (yellow, square), and C16-20k (blue, reverse triangle).

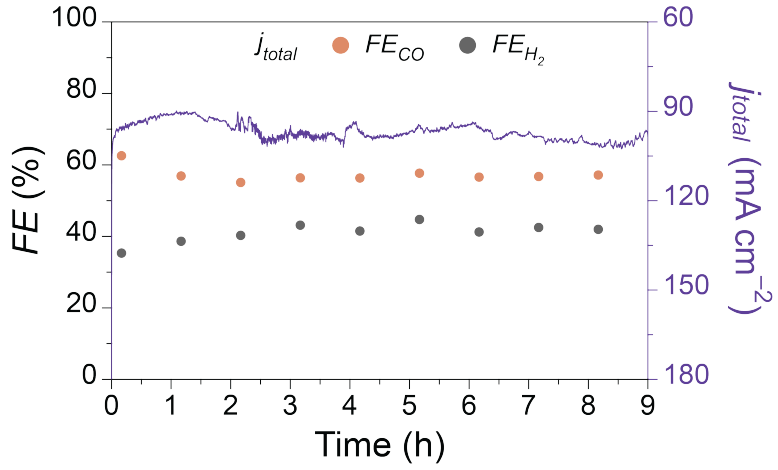

Figure S16. Long-term performance and durability of the CEM-based MEA containing representative C16-20k ionomer. The electrolysis was performed for 9 h at a cell voltage of 3.0 V using 0.1 M $KHCO_3$ as an anolyte. The electrode containing C16-20k maintained stable performance throughout the 9-h electrolysis.

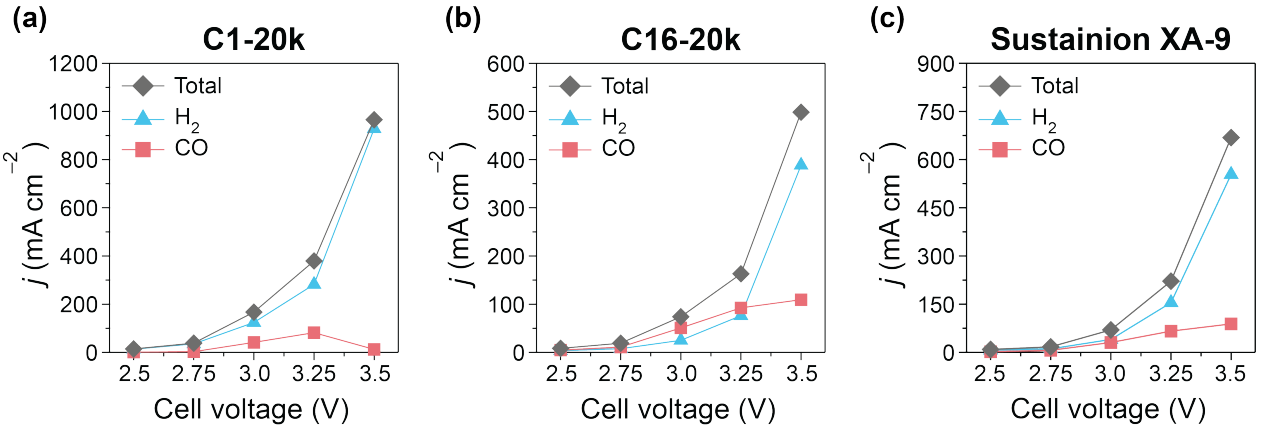

Figure S17. j_{total}, j_{H_2}, and j_{CO} for Ag-based electrodes coated with different ionomers in an MEA electrolyzer using a Nafion 211 membrane: (a) C1-20k, (b) C16-20k, and (c) Sustainion XA-9 ionomer. Measurements were conducted at cell voltages from 2.5 V to 3.5 V using 0.1 M $KHCO_3$ as an anolyte.

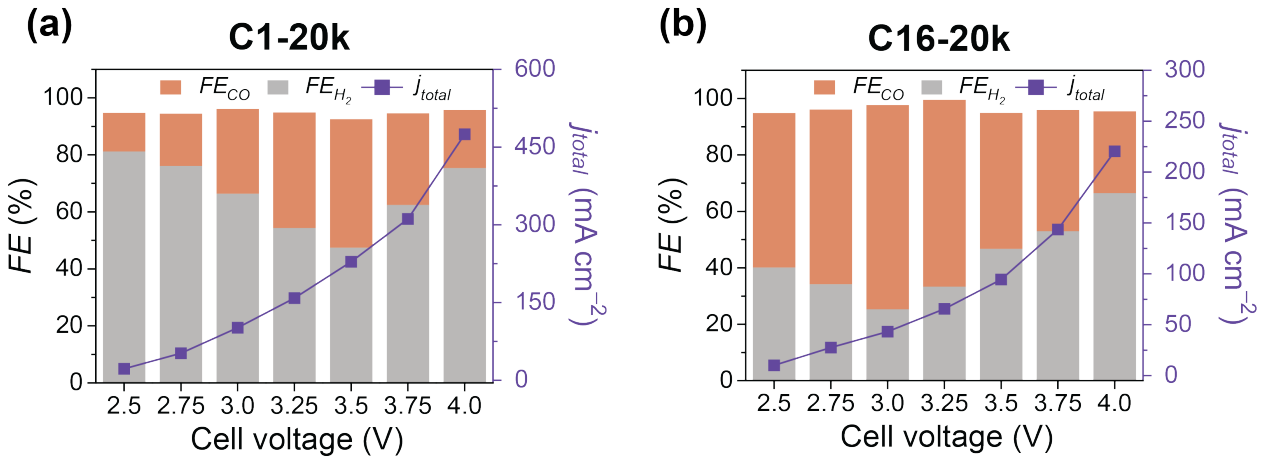

Figure S18. FE_{CO} and FE_{H_2} (left y-axis) and j_{total} (right y-axis) for Ag electrodes coated with different ionomers in an MEA using a PiperION membrane: (a) C1-20k, (b) C16-20k. Measurements were conducted at cell voltages from 2.5 V to 4.0 V using 0.1 M $KHCO_3$ as an anolyte. A 20 μm-thick PiperION self-supporting AEM was used after soaking in 1 M KOH for 24 h.

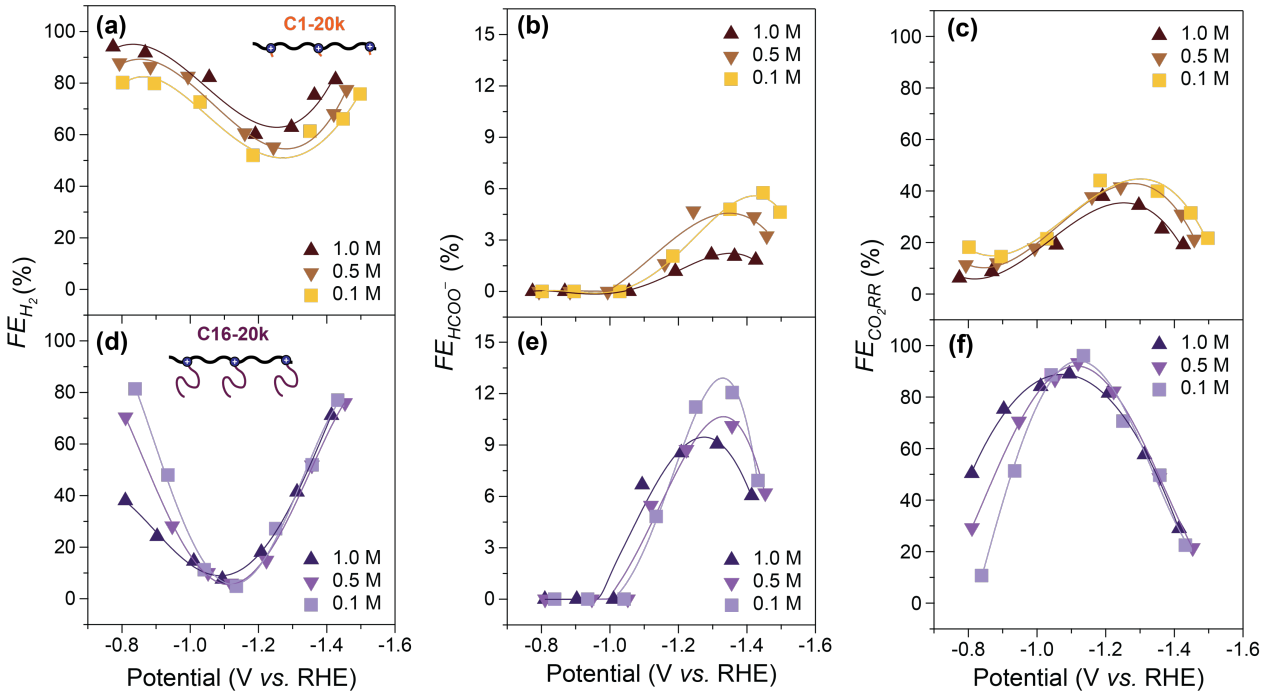

Figure S19. FE_{H_2}, FE_{HCOO^-}, and FE_{CO_2RR} on Ag-based electrodes coated with 1-*n*-alkylimidazolium ionomers in electrolytes with different HCO_3^- concentrations. (a–c) C1-20k and (d–f) C16-20k ionomers were evaluated in 1.0 M (triangle), 0.5 M (inverted triangle), and 0.1 M (square) HCO_3^- electrolytes. Insets depict the molecular structures of the respective ionomers.

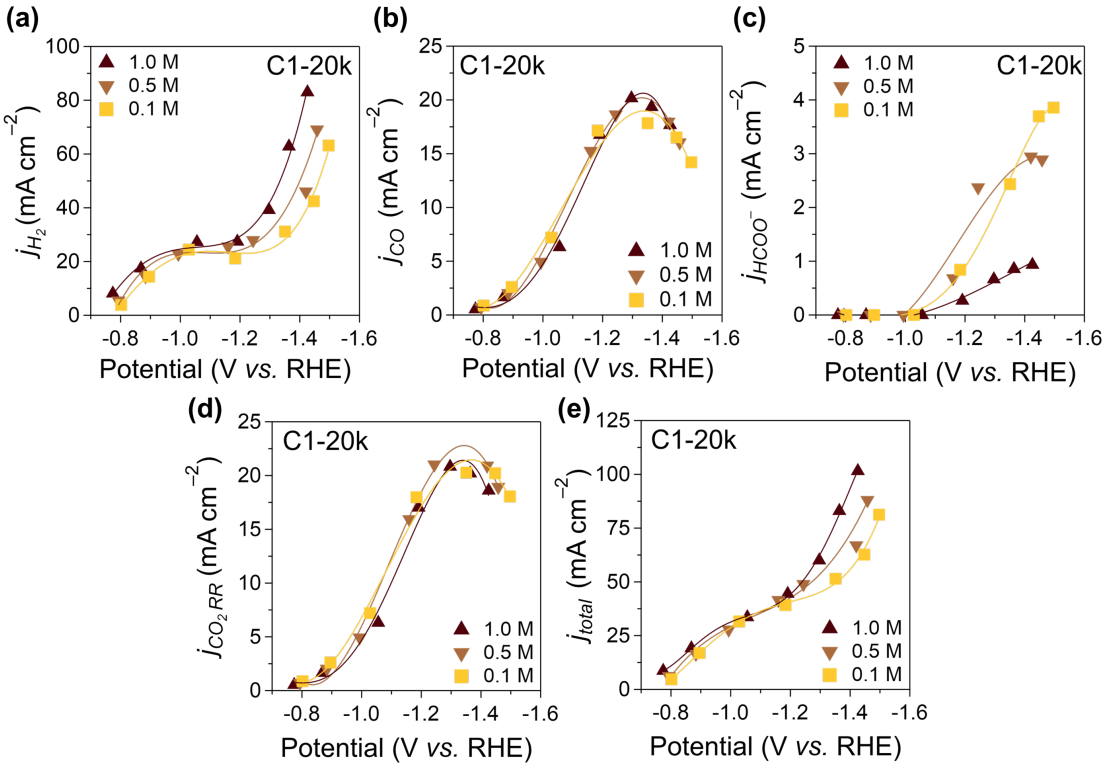

Figure S20. Effect of varying HCO_3^- concentrations (1.0 M, 0.5 M, and 0.1 M) on partial current densities (j) on Ag-based electrodes coated with the C1-20k ionomer: (a) j_{H_2}, (b) j_{CO}, (c) j_{HCOO^-}, (d) j_{CO_2RR}, and (e) j_{total}.

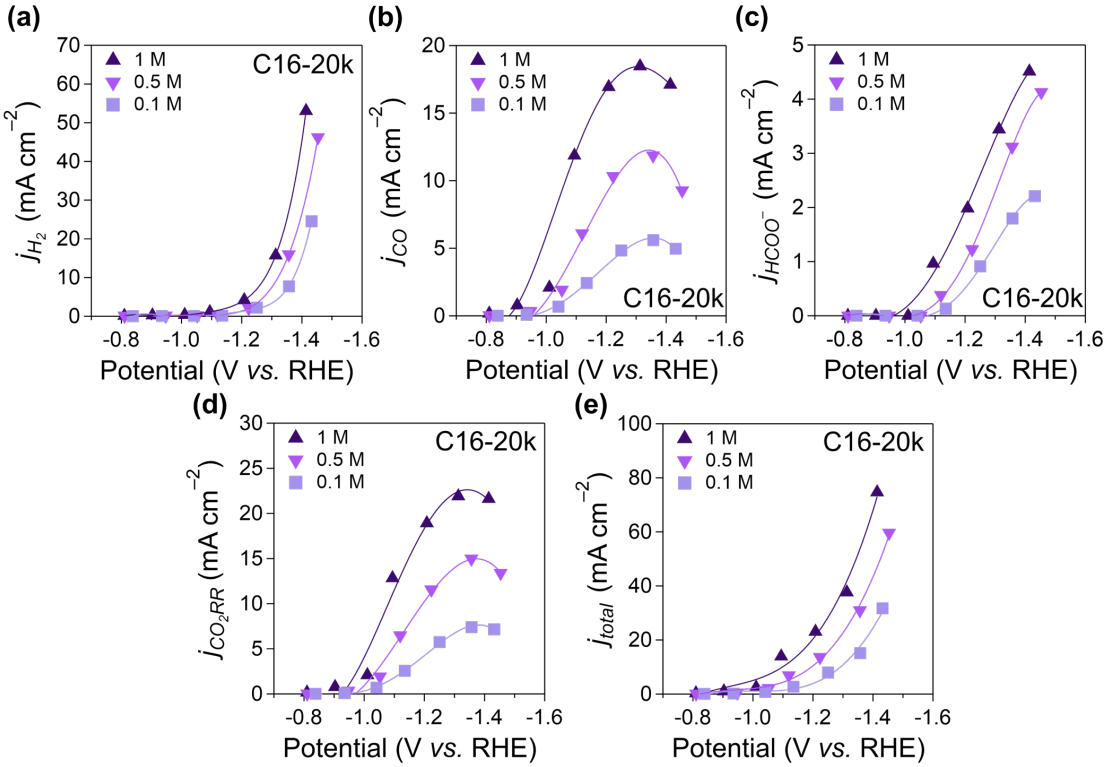

Figure S21. Effect of varying HCO_3^- concentrations (1.0 M, 0.5 M, and 0.1 M) on partial current densities (j) on Ag-based electrodes coated with the C16-20k ionomer: (a) j_{H_2}, (b) j_{CO}, (c) j_{HCOO^-}, (d) j_{CO_2RR}, and (e) j_{total}.

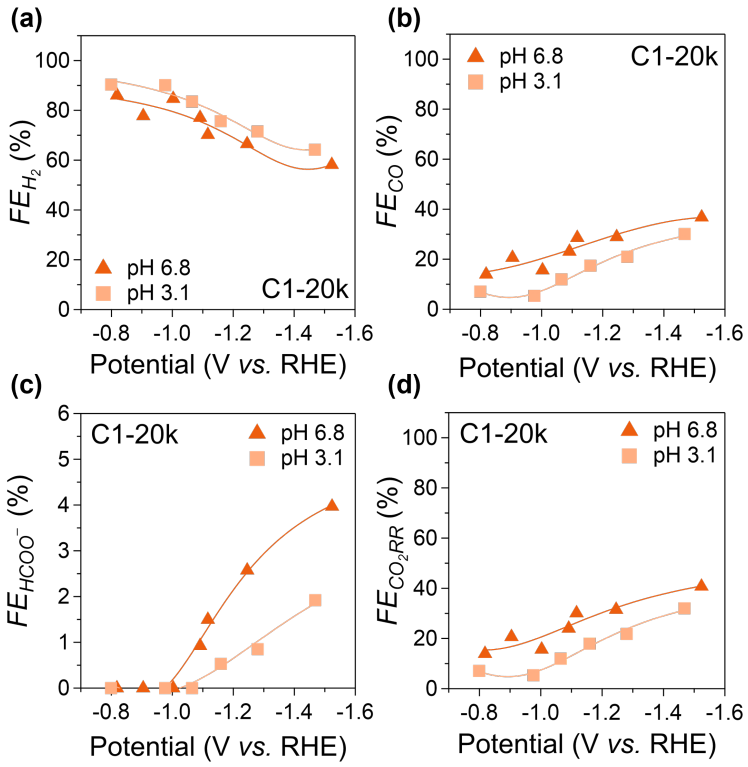

Figure S22. Effect of varying electrolyte pH (pH 6.8 and 3.1) on FE on Ag-based electrodes coated with the C1-20k ionomer: (a) FE_{H_2}, (b) FE_{CO}, (c) FE_{HCOO^-}, and (d) FE_{CO_2RR}.

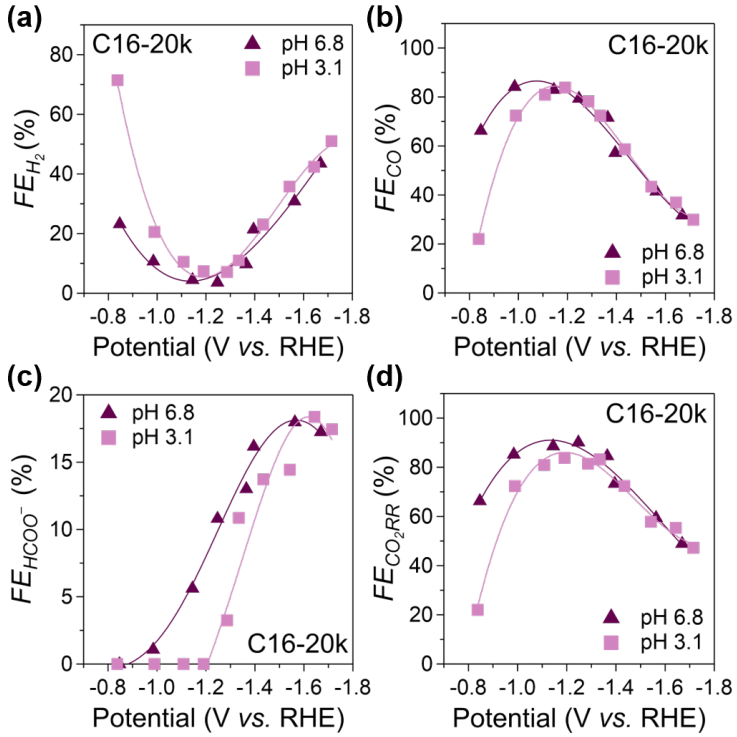

Figure S23. Effect of varying electrolyte pH (pH 6.8 and 3.1) on FE on Ag-based electrodes coated with the C16-20k ionomer: (a) FE_{H_2}, (b) FE_{CO}, (c) FE_{HCOO^-}, and (d) FE_{CO_2RR}.

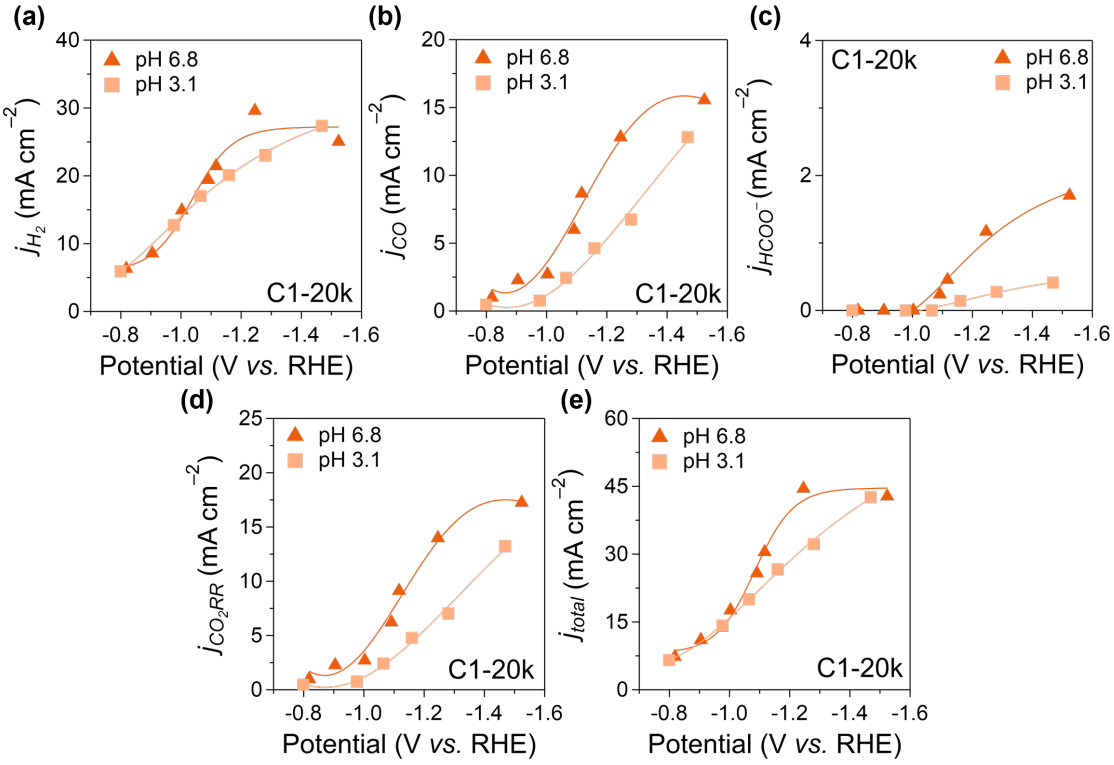

Figure S24. Effect of varying electrolyte pH (pH 6.8 and 3.1) on current densities (j) on Ag-based electrodes coated with C1-20k ionomer: (a) j_{H_2}, (b) j_{CO}, (c) j_{HCOO^-}, (d) j_{CO_2RR}, and (e) j_{total}.

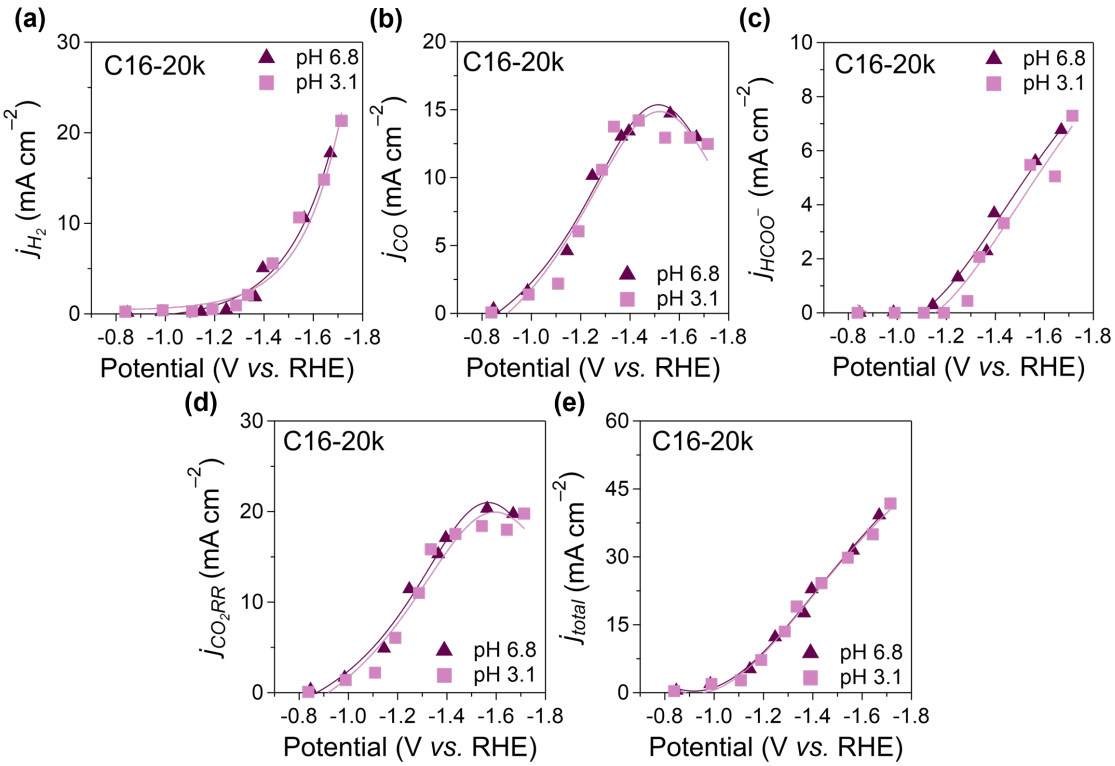

Figure S25. Effect of varying electrolyte pH (pH 6.8 and 3.1) on current densities (j) on Ag-based electrodes coated with C16-20k ionomer: (a) j_{H_2}, (b) j_{CO}, (c) j_{HCOO^-}, (d) j_{CO_2RR}, and (e) j_{total}.

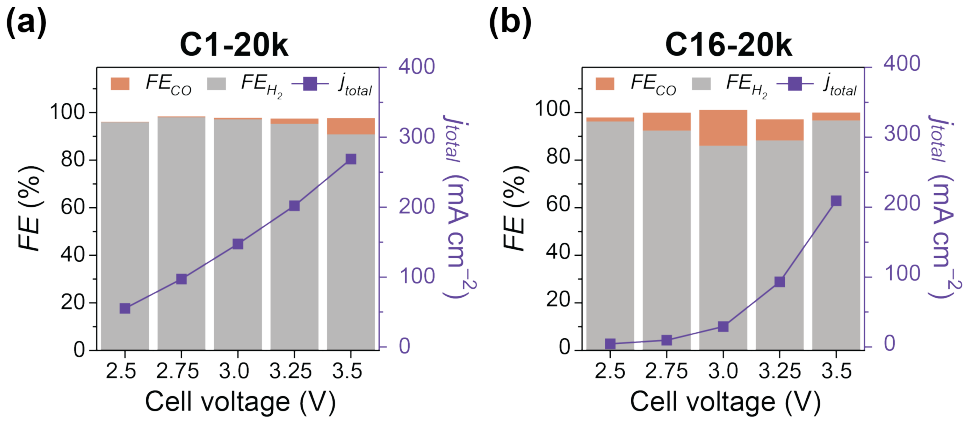

Figure S26. FE_{CO} and FE_{H_2} (left y-axis) and j_{total} (right y-axis) for Ag-based electrodes coated with different ionomers in a MEA fed with pure water using a Nafion 211 membrane: (a) C1-20k, (b) C16-20k. Measurements were conducted at cell voltages from 2.5 V to 3.5 V using deionized H_2O as an anolyte.

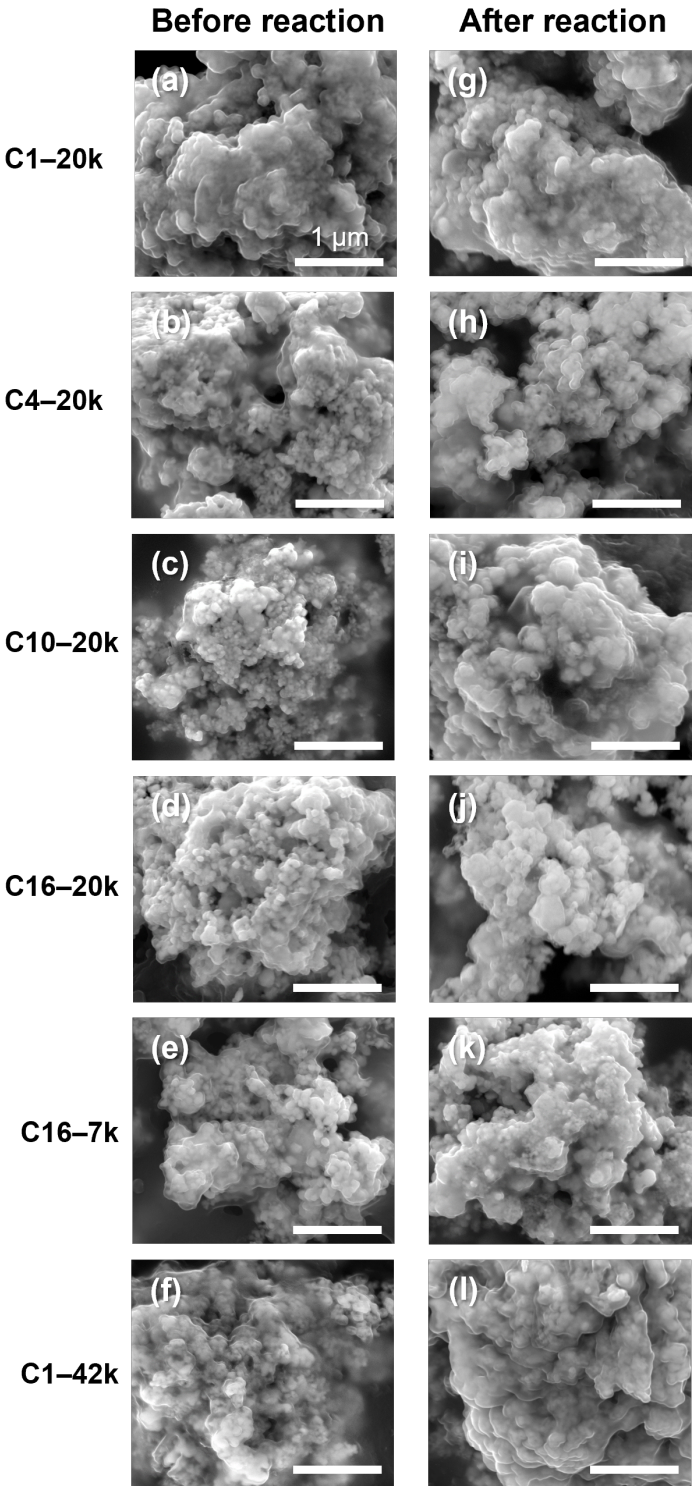

Figure S27. SEM images of all the electrodes used in this study: (a-f) before and (g-l) after CO_2RR

3. References

(S1) Chen, M.; Moad, G.; Rizzardo, E. Thiocarbonylthio end group removal from RAFT-synthesized polymers by a radical-induced process. *J. Polym. Sci. A Polym. Chem.* **2009**, *47*, 6704–6714.

(S2) Cheng, J.-Y.; Chu, Y.-H. 1-Butyl-2,3-trimethyleneimidazolium bis(trifluoromethylsulfonyl)imide ([b-3C-im][NTf_2]): a new, stable ionic liquid. *Tetrahedron Lett.* **2006**, *47*, 1575–1579.

(S3) Kutz, R. B.; Chen, Q.; Yang, H.; Sajjad, S. D.; Liu, Z.; Masel, I. R. Sustainion imidazolium-functionalized polymers for carbon dioxide electrolysis. *Energy Technol.* **2017**, *5*, 929–936.

(S4) Park, J.; Kim, E.-D.; Kim, S.; Lim, C.; Kim, H.; Ko, Y.-J.; Choi, J.-Y.; Oh, H.-S.; Lee, W. H. Deriving an efficient and stable microenvironment for a CO_2 MEA electrolyzer by reverse osmosis. *ACS Energy Lett.* **2024**, *9*, 3342–3350.

(S5) Resasco, J.; Chen, L. D.; Clark, E.; Tsai, C.; Hahn, C.; Jaramillo, T. F.; Chan, K.; Bell, A. T. Promoter Effects of Alkali Metal Cations on the Electrochemical Reduction of Carbon Dioxide. *J. Am. Chem. Soc.* **2017**, *139*, 11277–11287.